Chapter 12
Suitable Thermochemical Conversion Technology for Organic Waste Recovery in Developing Countries

Mohamed Asbik (ID)**, Toufik Boushaki** (ID)**, Veronica Belandria** (ID)**,
Stéphane Bostyn** (ID)**, and Brahim Sarh** (ID)

Nomenclature and AbbreviationsAbbreviations

AC	Activated Carbon
AFR	Air-Fuel Ratio
BET	Brunauer, Emmett et Teller theory
DE	Densification Energy ratio
DHW	Domestic Hot Water
EY	Energy efficiency
E_a	Activation Energy
FAR	Fuel-Air-Ratio
FC	Fixed Carbon
HHV	High Heat Value
HTC	HydroThermal Carbonization
k	Heating rate
LHV	Low Heat Value
m	Mass (or flow rates)
MC	Moisture content
MGW	Municipal green waste
OP	Olive Pomace
PW	The Process Water
R	Gas constant
R_0	Hydrothermal severity
SI	Severity Index

M. Asbik (✉)
Thermal and Energy Research Team (TERT), ENSAM, Mohammed V University in Rabat, Rabat, Morocco
e-mail: mohamed.asbik@ensam.um5.ac.ma

T. Boushaki · V. Belandria · S. Bostyn · B. Sarh
ICARE-CNRS, 1C Avenue de la recherche scientifique, Orléans Cedex 2, France

T   Temperature
t   Time
VM   Volatile Matter

Greek Symbols

λ   Air factor
Φ   Equivalence ratio
ω   Empirical parameter

Subscripts

0   Reference
a   Air
b   Burnout
c   Combustible/Fuel
i   Ignition
max   Maximum rate of mass loss
s   Stoichiometric conditions

12.1   Introduction

In the future decades, developing countries will be confronted with rising fossil fuel prices and climate change. To adequately and coherently overcome these challenges, they will certainly need an energy transition and resilient pathways through which they can achieve economic growth. This transition needs to promote clean and energy-saving (or energy-efficient) technologies, especially those of renewable resources (solar, wind, and hydropower) and biomass. Bioenergy is the largest form of renewables in use today. It is used in the industrial and transportation sectors, as well as for heating, cooking, and power generation through appropriate technologies (combustion and/or gasification). In developing countries, biomass and various wastes are abundant renewable resources that could reduce greenhouse gas emissions when used in efficient conversion systems compared to fossil fuels. Furthermore, the use of these products would increase farm incomes and improve soil quality. The competitiveness of biomass energy depends mainly on conversion system technologies and the availability of low-cost feedstocks, such as straw, crop waste, and agricultural or forestry residues. For these reasons, capacity factors for bioenergy plants are varied. Thus, between 2010 and 2019, the global

Table 12.1 Evolution of solid biomass use for energy in the IEA bioenergy member countries and comparison with the domestic forest areas

Country	GJ solid biomass/capita				GJ/hectare forest (2019)
	2005	2010	2015	2019	
Brazil	9.86842	12.23684	12.85088	13.24561	7.41176
China	4.82456	3.46491	2.80702	2.80702	21.41176
India	4.84277	5.72327	5.34591	5.59748	132.58824
South Africa	6.28931	6.79245	5.59748	5.59748	19.76471
Sweden	33.33333	39.90826	38.3792	40.21407	14.82353
USA	7.03364	6.88073	6.88073	7.49235	8.23529
EU28	6.72783	8.7156	9.02141	9.78593	32.11765

Adapted from IEA bioenergy countries' Report-update 2021 (Pelkmans 2021)

weighted-average capacity factor for bioenergy projects ranged from a low of 65% in 2012 to a high of 86% in 2017 (IRENA 2020). In 2019, the levelized cost of electricity (LCOE) ranged from a low of 0.057\$/kWh in India and 0.059\$/kWh in China to 0.08\$/kWh in Europe and 0.099\$/kWh in North America (IRENA 2020).

To clarify expectations, the solid biomass potential is presented in Table 12.1. This category of organic waste consists of wood and its derivatives and agricultural residues such as bagasse and straw. It remains the dominating type of biomass used for energy in all countries which have a high domestic forest area per capita and considerable wood processing industries. It shows that the highest energy levels from solid biomass (per capita) are reached in Sweden (developed country), whereas developing countries (Brazil, China, India, and South Africa), the USA, and the European Union (EU28) have low energy levels. The last right column of Table 12.1 also exhibits the amount of solid biomass used for energy in 2019 in terms of domestic forest areas.

The organic wastes conversion is quite often carried out by using different thermochemical conversions, namely pyrolysis, torrefaction, combustion, gasification, and hydrothermal carbonization

12.2   Organic Wastes Characterization

The conversion of energy from biomass to other forms of energy needs the knowledge of the physicochemical properties of each biomass predisposed to be a candidate for the chosen conversion technology. This technology could account for differences in the physical characteristics of the biomass and the proximate composition which can vary greatly in terms of moisture and ash content. Moreover, many conversion technologies are in need of ultimate analysis (elemental composition or elemental (C, H, N, S, O)) too (D. Yogi Goswami and Kreith 2008).

12.2.1 Physicochemical Properties of Biomass

12.2.1.1 Physical Characteristics

Bulk density and particle size are the two major physical properties that should be considered in designing conversion systems for biomass handling. The bulk density of a biomass is influenced by the size, shape, moisture content, particle density, and surface characteristics. For example, hollow wheat straw particles have wet and dry density bulk ranging from 24 to 111 kg.m^{-3}. This biomass is composed of cylindrical shape particles whose lengths range from 6 to 50 mm and moisture content varies from 8% to 60% wet basis (w.b) (Lam et al. 2008).

12.2.1.2 Chemical Characteristics

The chemical properties of a biomass constrain the choice of the thermochemical conversion process. The most important characteristics of biomasses concern ultimate (or elemental) and proximate analyses.

Ultimate Analysis

The chemical elements of a solid biofuel (biomass) have varying concentrations according to their types and origins. In the organic phase, the ultimate (or elemental) analysis gives the composition of biomass essentially as weight percentages of six major elements, namely carbon (C), hydrogen (H), and oxygen (O) as well as nitrogen (N), sulfur (S), and chlorine (Cl) if any one of those elements exists. In fact, the Cl significant content is present in certain biomass materials like municipal and animal wastes, herbaceous biofuels, fruit residues, and grains. During thermochemical conversion, this element (Cl) can react with other elements to form chloridric acid (HCl), Cl_2, KCl, and NaCl. Consequently, it may be a possible pollutant and corrosive agent in combustion and gasification conversion processes.

It should be noted that American Standard Testing Methods (ASTM) is usually used to carry out the elemental analysis. Furthermore, this analysis is used to determine the empirical chemical formula of a biomass and allows for establishing models for predicting its higher heat value (HHV) (Vargas-Moreno et al. 2012). In order to clarify and elucidate that issue, Tables 12.2 and 12.4 display the ultimate analysis of olive pomace, argan nut shell, and miscanthus, respectively.

Table 12.2 Elemental analysis and high heat value of olive pomace and argan nut shell

Elemental analysis (%)	C (%)	H (%)	N (%)	S (%)	O (%)	HHV (MJ/kg)
Olive pomace (Elorf et al. 2016)	59	8.5	1.5	0	31	21.3
Argan nut shell (Rahib et al.; 2021)	51.33	6.32	0.005	0	42.35	20.6

Proximate Analysis

Chemical characteristics essentially concern proximate and ultimate analyses. In addition, proximate analysis covers the determination of moisture content (MC), volatile matter (VM), and ash (Ash). As for the calculation of the fixed carbon (FC), it is given by Eq. (12.1):

$$FC(\%) = 100 - \left[MC(\%) + Ash(\%) + VM(\%) \right] \tag{12.1}$$

The proximate analysis can be done by ASTM (American Society for Testing and Materials) methods (Milne et al. 1990), thermogravimetric analysis (TGA), or differential thermogravimetric (DTG) (Klass 1998).

Usually, the high heat value (HHV) is required with proximate analysis too. HHV of a fuel sample is the higher amount of heat released when a unit mass of the fuel is burned. It is measured using oxygen bomb calorimeter in which a specified mass of sample is burned under standardized conditions. As with ultimate analysis, Table 12.4 shows an example of proximate analysis of olive pomace (OP) and miscanthus.

12.2.2 *Types of Biomasses*

Lignocellulosic biomass is the oldest energy source after the sun. It is the most renewable organic material such as wood, crops, plants, and animal wastes. Biomass gets its energy from the sun via the photosynthesis process since sunlight provides plants with their energy needs to convert water and carbon dioxide into oxygen and sugars. Due to its unlimited supplies, biomass is considered a renewable energy source. Developing countries have a diversified and abundant potential biomass such as rice straw (China, India, Indonesia, …), sugarcane bagasse (Brazil, India, China, …), wheat straw (China, India, Argentina, …), and maize straw (China, Brazil, Mexico, South Africa, …).

12.3 **Gasification and Pyrolysis**

Pyrolysis and gasification are high temperature thermochemical conversion technologies for converting biomass and waste into gaseous fuel. Different technologies are used for this purpose including fixed bed, entrained flow, and fluidized bed.

In pyrolysis, when the organic material is subjected to an intense temperature gradient, under an inert atmosphere (argon), it decomposes producing gases (pyrolysis gases: H_2, CO, CO_2, CH_4, C_2H_4, C_2H_5, C_2H_6, C_6H_6, C_3H_4, C_3H_6, C_3H_8, C_4H_{10}, H_2S, C_7H_8, C_2H_5OH, C_2H_4O) (Elorf et al. 2021) and a solid product namely char and

tars (composed of a mixture of water and several hundred oxygenated organic compounds whose composition depends on the initial biomass) (Evans and Milne 1987).

Depending on the temperature and the heating rate, there are three types of pyrolysis:

- Slow pyrolysis (T = 350–600 °C and heating rate $k \leq 10$ °C/min).
- Fast pyrolysis (T = 600–800 °C, $10 \leq k \leq 50$ °C/min) generally is used to maximize the yield of liquid bio-oil products.
- Flash pyrolysis (T = 450–600 °C, $k \geq 50$ °C/min and residence time less than 1 s). Yields of flash pyrolysis oil can be as high as 60–70 wt.% under optimized conditions (Ighalo et al. 2022).

The heating rate has a great influence on the pyrolysis process. When it is high, it leads to the rapid formation of volatile matter with a high C/H ratio. Conversely, slow pyrolysis at low temperatures (between 300 and 400 °C) promotes char production.

During pyrolysis, temperature of biomass particles is highly variable. Certainly, the temperature rise is difficult to control because it is ruled by competitions between chemical kinetics and heat transfers. Heat transfers in the particle are subject to different parameters: particle size, humidity, thermal conductivity of the material, etc. Temperature and heat flux density have influence on the overall distribution of pyrolysis products. The geometry of the particles to be pyrolyzed is an important parameter if the size is too high and the residence time of the tars within the particles increases, which can cause the degradation of these tars via intraparticle secondary reactions. The mass yield of the pyrolysis products, which represents 30% of char, 30% of condensable, and 30% of gas, for a heat flux density less than 10 kW/m² and a temperature value less than 500 °C (primary pyrolysis), becomes approximately 60–75% of condensable for a heat flux density greater than 10 kW/m². When the temperature becomes greater than 700 °C (secondary pyrolysis), the gases represent more than a third of the products for a heat flux density <10 kW/m² and reach 80% of the pyrolysis products for heat flux density values >10 kW/m².

Pyrolysis is also a preliminary phase to gasification. When the oxidizing agent is present with limited quantity in the pyrolysis process, partial gasification is obtained. Conversely, when this oxidizing agent is present in sufficient quantity, the thermochemical process is a combustion phase.

12.3.1   Gasification

Like pyrolysis, gasification is a thermochemical process of converting biomass or waste into a mixture of combustible and non-combustible gases called syngas. This process takes place in a gasifier. The combustible fraction of syngas consists of methane (CH_4), carbon monoxide (CO), and hydrogen (H_2), and the non-combustible fraction consists of carbon dioxide (CO_2), moisture (H_2O), and nitrogen (N_2).

There are several types of gasifiers: moving bed gasifiers and fixed-bed gasifiers which can be classified as updraft, downdraft and double fire throated gasifiers, and bubbling or circulating fluidized bed gasifiers. Figure 12.1 provides a schematic view of some gasifier types.

The choice of gasification process type rests on several parameters such as the installation fuel consumption (in kg/h), power range (10–10,000 kW for fixed-bed gasifiers and 5–100 MW for fluidized-bed), the biomass or waste used, and the downstream gas application.

12.3.2 Fixed Bed Gasifiers

The first gasification technology that emerged is fixed-bed gasifiers. Fixed-bed processes are generally easy to make and operate. They are the most chosen for small-to medium-scale heat and power production. In updraft or downdraft fixed-bed gasifiers, the fuel, consisting of biomass or waste, forms a dense bed inside the reactor which moves vertically. Biomass is introduced at the top of the gasifier in updraft processes, the gasifying agent is introduced at the bottom, and syngas is recovered at the top. However, in a downdraft gasifier (Fig. 12.1b), the biomass is introduced at the top, as in an updraft gasifier, the gasifying agent is introduced in the middle at the level of the throat and the syngas is recovered at the bottom.

The gas produced in the updraft process is heavily laden with tar. The tar which forms during the pyrolysis phase flows upward to the cooler region. On the other hand, the downdraft process promotes tar cracking. Indeed, tar production is low because the tar produced during the pyrolysis phase crosses the combustion zone and a large part is converted. Nevertheless, to produce gas without tar or with very small quantities of tar, a cleaning system must be provided.

Finally, it can be noted that fixed bed gasifiers support large particles. The particles constituting the fuel can have a dimension ranging between 2 and several millimeters. The residence time required for gasification is counted in hours.

12.3.3 Bubbling and Circulating Fluidized Bed Gasifiers

The other category of gasifier is bubbling fluidized bed gasifiers (Fig. 12.1c) and the circulating fluidized bed (Fig. 12.1d) which suits for the medium and large scale and for which the particle sizes is limited up to 20 mm that needs the grinding of the raw material. This process requires higher fluidized bed velocity to suspend the particle bed (Grace et al. 2006) and produce a high level of mixing between biomass and bed material which makes it possible to achieve a biomass thermal conversion system of around 96% (Sansaniwal et al. 2017). This is due to the partial oxidation of most of the carbon contained in the biomass. As a result, smaller amounts of tar are generated (no more than 20 g/mm^3 for bubbling and 5 g/mm^3 for circulating fluidized bed) (Valderrama Rios et al. 2018).
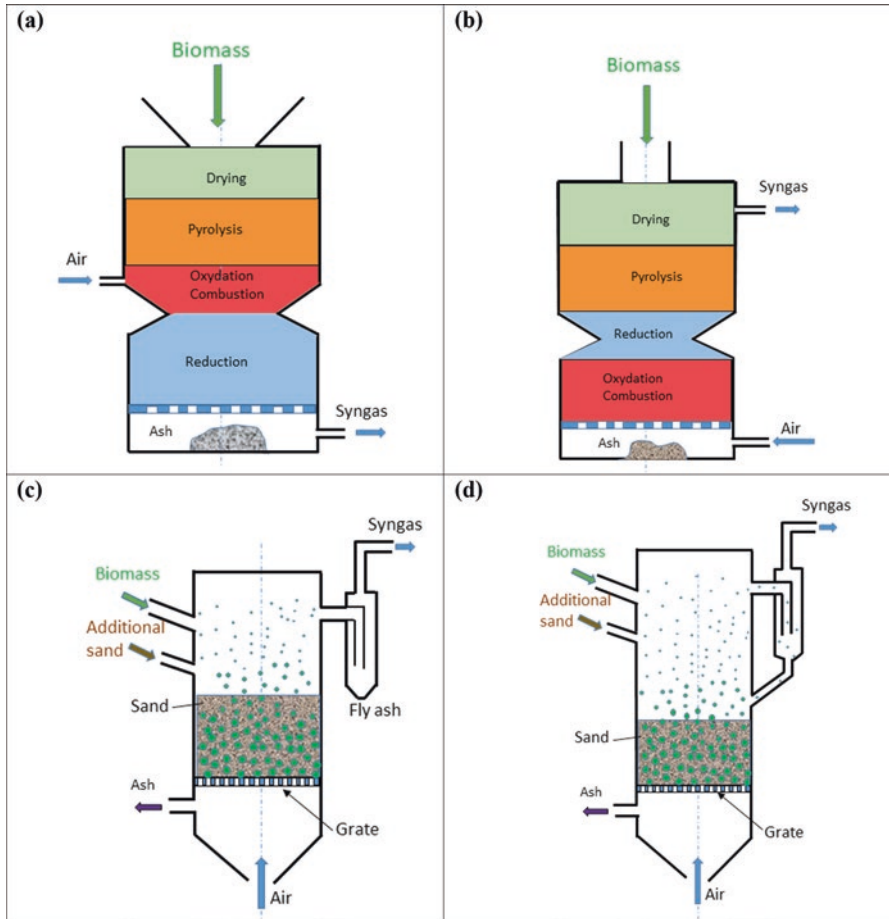
Fig. 12.1 Schematic of gasifiers: Fixed bed [(**a**) downdraft, (**b**) updraft], (**c**) bubbling fluidized bed, (**d**) circulating fluidized bed
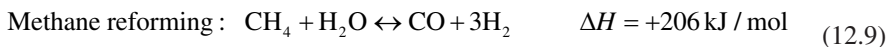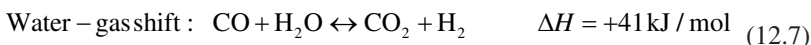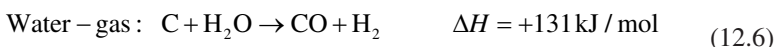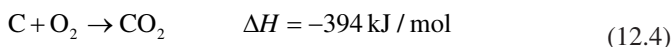
12.3.4 Gasification Process

In a gasifier, the gasification process generally involves four phases:

- Drying in which the moisture content in the biomass or waste is vaporized and humidity is converted into steam. This step takes place up to a temperature of about 200 °C so that the moisture content drops below 20%, allowing the favorable moisture condition for gasification to be reached.
- Pyrolysis is in which biomass components are decomposed into volatile compounds (gas pyrolysis and tar) and solid residues (char).

- Oxidation or partial combustion takes place in the presence of a gasifying agent. In the gasification process, the oxygen quantity is lower than the theoretical requirement in the combustion process.
- Reduction or gasification occurs in the presence of other gasifying agents such as CO_2 and water vapor.

These phases entail reactions that happen at the same time in the gasification process (Watson et al. 2018). The main reactions in this zone during the air gasification process are as follows (Gai and Dong 2012; Mandl et al. 2010; Patra and Sheth 2015):

$$\text{Pyrolysis}: \quad CH_xO_y \rightarrow Tar + Char + Gases\left(H_2; CO; CH_4; CO_2; H_2O; C_nH_m\right) \quad (12.2)$$

$$\text{Oxidation}: \quad C + 0.5O_2 \rightarrow CO \qquad \Delta H = -111\,kJ/mol \quad (12.3)$$

$$C + O_2 \rightarrow CO_2 \qquad \Delta H = -394\,kJ/mol \quad (12.4)$$

$$\text{Boudouard}: \quad C + CO_2 \leftrightarrow 2CO \qquad \Delta H = +172\,kJ/mol \quad (12.5)$$

$$\text{Water} - \text{gas}: \quad C + H_2O \rightarrow CO + H_2 \qquad \Delta H = +131\,kJ/mol \quad (12.6)$$

$$\text{Water} - \text{gas shift}: \quad CO + H_2O \leftrightarrow CO_2 + H_2 \qquad \Delta H = +41\,kJ/mol \quad (12.7)$$

$$\text{Methanation}: \quad C + 2H_2 \leftrightarrow CH_4 \qquad \Delta H = -75\,kJ/mol \quad (12.8)$$

$$\text{Methane reforming}: \quad CH_4 + H_2O \leftrightarrow CO + 3H_2 \qquad \Delta H = +206\,kJ/mol \quad (12.9)$$
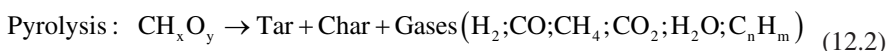
In the gasification process, where several reduction reactions occur, the gas production is impacted by the reaction temperature. Endothermic reactions are thus favored when the temperature increases, which improves the process.

12.3.5 Gasification Modeling

In the gasification process, the reactions generated are complex and factors such as moisture content, biomass feedstock composition and operating parameters (temperature, pressure, air/biomass ratio, etc.) have an important effect on the gas produced. To understand the effect of each parameter on the performance of gasification systems, mathematical modeling for the gasification process has developed (kinetic models, artificial neural networks, CFD, thermodynamic equilibrium model) (Silva et al. 2019). In the stoichiometric equilibrium model, the chemical reaction equilibrium constant method is used, while the non-stoichiometric equilibrium model uses Gibbs free energy minimization. Note that the equilibrium approach is independent

of the gasifier design. In the kinetic models, the reaction kinetics and species transport equations are solved, and the temperature and composition profiles of the products at different positions along the gasifier are described. In computational fluid dynamics (CFD), mass, momentum, energy, and species transport conservation equations, turbulence models, and multiphase flow models in a space-time domain of a gasifier are solved for the prediction of temperature and concentration profiles in all regions of the gasifier.

12.4   Biomass Combustion

Combustion is the thermochemical process intended to produce heat directly. Ligneous biomass is made up of forest or agri-food residues: bark, branches, straw, sawdust, wood pellets, etc. It is used as fuel to supply a boiler, a hot air generator, or a wood oven. Thus, this primary energy is used to obtain hot water, hot air, or steam. Steam is used, among other things, to produce electricity.

The use of biomass as an energy source contributes to the natural carbon cycle; the amount of carbon dioxide (CO_2) released into the atmosphere during the combustion corresponds to that absorbed by the biomass by photosynthesis. Sectors that do not require significant energy consumption to grow and process raw biomass have a favorable CO_2 balance.

Energy recovery from wood and biomass is the leading source of renewable energy in France and Europe. In the latter, wood and biomass represent approximately 65% of renewable energy consumption and in France just over 50%, including 75% of thermal energy (the second renewable energy is hydropower, used to produce electricity) (Rogaume 2009). Even though numerous research and development works aimed at developing new ways of energy recovery (pyrolysis, gasification, liquefaction, etc.), more than 95% of the current recovery is carried out by direct combustion in plants whose power and technology vary considerably. Besides, among the biomasses of plant origin, wood is the vast majority of these systems.
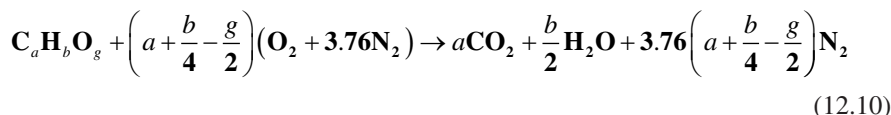
12.4.1   Principle of Biomass Combustion

Biomass combustion is a complex process that includes transfers of heat and matter and reactions in homogeneous and heterogeneous phases. Its main stages are as follows (Nussbaumer 2003; Rosendahl 2013):

– Drying
– Pyrolysis
– Oxidation reactions in the gas phase
– The gasification/combustion of char

During the heating of biomass, its constituents are hydrolyzed, oxidized, dehydrated, and pyrolyzed as temperature increases, forming condensable and noncondensable volatile species, as well as coal with high carbon content. At the ignition temperature of the volatile species and in the presence of oxygen, exothermic reactions (combustion) are triggered. The major combustion products (CO_2 and H_2O) can also react with the residual char during its oxidation.

The stoichiometric combustion (ideal combustion) of a $C_\alpha H_\beta O_\gamma$ hydrocarbon with air can be expressed by the following equation:

$$\mathbf{C_a H_b O_g} + \left(a + \frac{b}{4} - \frac{g}{2} \right) \mathbf{(O_2 + 3.76N_2)} \rightarrow a\mathbf{CO_2} + \frac{b}{2}\mathbf{H_2O} + \mathbf{3.76} \left(a + \frac{b}{4} - \frac{g}{2} \right) \mathbf{N_2}$$

(12.10)

The coefficients associated with each species in Equation (12.10) (marked in **bold**) are called stoichiometric reaction coefficients. The amount of air needed to burn a stoichiometric mixture is called stoichiometric or theoretical air. The approximate standard composition of dry air is about 21% oxygen and 79% nitrogen, hence the value of 3.76.

In fact, the combustion is non-stoichiometric, i.e., the fuels are often burned with a quantity of air different from the theoretical ratio. If less than the stoichiometric air is used, the mixture is described as rich in fuel. If excess air is used, the mixture is considered as lean in fuel. For this reason, it is convenient to quantify the combustible mixture using the two main relations: equivalence ratio (ER or Φ) and fuel-air ratio (FAR).

The air-fuel ratio, AFR, is defined as the mass of air supplied to a combustion system per unit mass of fuel during combustion, namely:

$$\text{AFR} = \frac{\text{Air used}\,(\text{kg / time unit})}{\text{fuel used}\,(\text{kg / time unit})} = \frac{m_a}{m_c}$$

(12.11)

where m_a and m_c are the respective masses (or flow rates) of air and fuel.
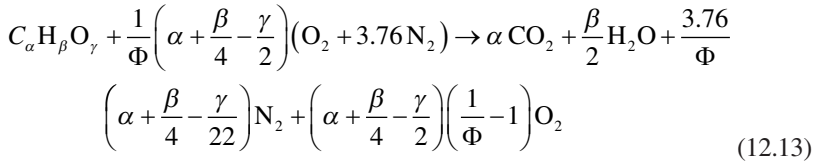
The inverse of AFR is also used, fuel-to-air ratio, **FAR = 1/AFR.** The equivalence ratio (Φ) of a system is defined as the ratio of the real fuel-to-oxidizer ratio to the stoichiometric fuel-to-oxidizer ratio. Mathematically,

$$\Phi = \frac{\text{FAR}_{real}}{\text{FAR}_s}$$

(12.12)

The subscript "s" indicates a value under stoichiometric conditions. For Φ < 1, the mixture is considered lean; for Φ = 1, the mixture is stoichiometric; and for Φ > 1, the mixture is considered rich. The inverse of Φ is also used, air factor, **λ = 1/Φ.**

Generally, combustion products include many different species in addition to the main species (CO_2, H_2O, N_2, O_2). The equilibrium of the stoichiometric equation

requires the use of thermodynamic equilibrium relations. If the combustion products contain only major species (complete combustion) and excess air, the overall lean combustion equation ($\Phi < 1$) is written as follows:

$$C_\alpha H_\beta O_\gamma + \frac{1}{\Phi}\left(\alpha + \frac{\beta}{4} - \frac{\gamma}{2}\right)(O_2 + 3.76\,N_2) \rightarrow \alpha\,CO_2 + \frac{\beta}{2}H_2O + \frac{3.76}{\Phi}$$

$$\left(\alpha + \frac{\beta}{4} - \frac{\gamma}{22}\right)N_2 + \left(\alpha + \frac{\beta}{4} - \frac{\gamma}{2}\right)\left(\frac{1}{\Phi} - 1\right)O_2$$

$$(12.13)$$

As a result of the combustion process, different types of pollutants can be distinguished:

– Unburnt pollutants such as CO, $C_X H_Y$, PAH, tar, soot, unburnt carbon, H_2, HCN, NH_3, and N_2O
– Pollutants from complete combustion such as NO_x (NO and NO_2), CO_2, and H_2O
– Ash and contaminants such as ash particles (KCl, etc.), SO_2, HCl, PCDD/F, Cu, Pb, Zn, Cd, ...

12.4.2   Used Technologies

Burning waste is an old process that reduces its volume and recovers energy. The mastery of this technology in a closed fireplace is much more recent. Indeed, the first urban waste incinerators date back to the beginning of the last century in Europe. This technology then developed with the inexorable increase in the quantity of urban waste throughout the twentieth century. It makes it possible to reduce the volume of this waste by around 90%, recover energy from this waste, and restrict landfilling to final waste only.

Energy recovery from biomass through combustion has benefited from the development of the thermal waste treatment chain. This processing chain is made up of five elements:

1. The combustion equipment supply system
2. The combustion equipment (furnace, burner)
3. A possible energy recovery system
4. A flue gas analysis and treatment device
5. A storage space for solid residues after combustion

The varying shapes and characteristics of the solids to be burned require different combustion plants. The most used technologies are (Tillman 1987) the following:

– Grate kilns
– Fluidized bed kilns
– Rotary kilns
– Pulverized carbon kilns

The grate kiln is the most used incineration process for urban waste. The block diagram is shown in Fig. 12.2. Generally, the combustion zone can be divided into three parts as shown in Fig. 12.2. The distribution of the primary air under the grate is done by means of boxes, the number of which varies according to the installations.

For units with a high treatment capacity, it is generally a furnace-boiler assembly. Several types differ in shape, size, or even the inclination of the grid, thus giving different movements to the waste. Grid dimensions depend on the heat value of the fuel and the load

12.4.3 Technical Issues Related to Biomass Combustion

Three main phenomena can occur during the combustion of biomass and affect the operation of the combustion equipment used, or even damage it: the formation of bottom ash, the fouling of the heat exchange zones, and corrosion (Demirbas 2007; Khan et al. 2009; Sommersacher et al. 2012).

12.4.3.1 Formation of Bottom Ash

Bottom ash is a pile of partially melted ash. The bottom ash formation process is associated with the phenomenon of sintering (agglomeration of particles under heat effect) and partial melting of ash particles. Bottom ash deposit on a burner for pulverized biomass boilers can cause burner ignition problems or other operational difficulties and affect combustion performance. On the heat exchange surfaces of the combustion chamber, the bottom ash reduces the heat absorption capacity of the furnace. Among the compounds that promote the formation of bottom ash, we can
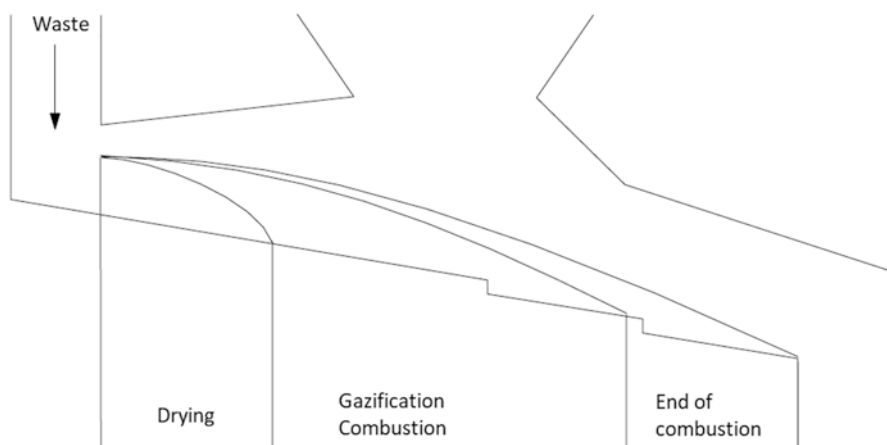

Fig. 12.2 Schematic diagram of a grate kiln

mainly mention alkalis, mainly potassium (K) and sodium (Na), silica (Si), sulfur (S), and chlorine (Cl).

The design of the boiler/furnace can limit the appearance of bottom ash. Temperature close to the combustion chamber wall should, for example, be low enough to avoid the melting of ash on these walls, the starting point for the formation of bottom ash.

12.4.3.2   Fouling of Heat Exchange Zones

Ash deposition "fouling" can occur in the convection zones of boilers on the heat exchange surfaces where the temperature of the flue gases decreases. This causes the reduction of heat absorption capacity of the convection zones of the boilers and an increase in the gas outlet temperature. If the fouling is severe, it can increase the pressure drop in the heat exchanger tubes. The main technical means of destroying ash deposits in convective zones is the use of compressed air or steam guns, which by mechanical impact and thermal shocks allow the breaking of deposits to eliminate them.

12.4.3.3   Corrosion

The corrosion is caused by different mechanisms: the direct attack of gaseous HCl or Cl2 on the heat exchange surfaces; the formation of chloride and/or alkaline sulfate deposits, which dissolve the oxide layer protecting the heat exchange surfaces; and the sulfation of chlorides of alkali metals and heavy metals deposited on the exchange tubes, which results in the release of Cl, which can then attack the surface of the tube and lead to its corrosion. Among the technical solutions to prevent corrosion, we can mention the use of specific alloys or coatings. Lowering the temperature of the water or water vapor in the heat exchange tubes also makes it possible to reduce the temperature of their metal surface and thus reduce the rate of corrosion.

12.4.4   Biomass Combustion: CNRS-ICARE Boiler

12.4.4.1   Experimental Setup

As part of the VERA 2015–2018 project (France – Morocco), we developed a biomass boiler (Fig. 12.3) for the combustion of agricultural residues, and, in particular, olive pomace and argan nut shells. The biomass supply is done by the supply tank (biomass storage hopper) and an endless screw to convey the fuel inside the chamber. In the boiler, the biomass is distributed with a rotating leveler at the bottom of the chamber. The air supply is done by a fan driven by a variable speed motor and, therefore, an adjustable airflow after calibration. The flame develops vertically along the chamber; the combustion products pass through a cyclone and then a
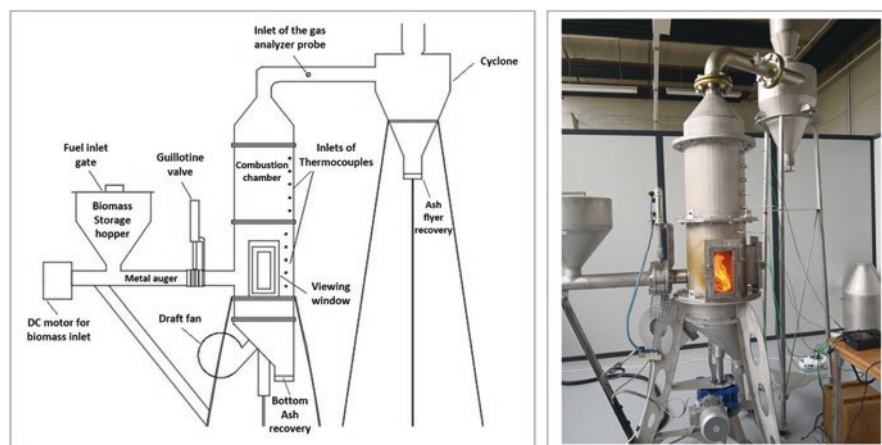
Fig. 12.3 VERA biomass boiler developed at ICARE-CNRS, diagram of the entire installation (left), photo of the boiler (right)

Table 12.4 Properties of selected biomass materials

	OP	Miscanthus
Proximate analysis (%)		
MC	7.4	9.8
VM	74.2	69.4
FC[a]	16.1	20.4
Ash	2.3	0.4
Ultimate analysis (%)		
Carbon	53.5	53.4
Hydrogen	6.8	4.4
Nitrogen	1.1	0.48
Sulfur	–	0.3
Oxygen[a]	38.6	41.3
HHV[b] (MJ/kg)	22.5	16.8

Jayaraman and Gökalp (2015) and Missaoui et al. (2017a, b)
MC moisture content, *VM* volatile matter, *FC* fixed carbon
[a]By difference
[b]Higher heating value

smoke scrubber to remove particles and possibly odors. The boiler has a viewing window, full-height thermocouples, and a multi-gas analyzer installed at the chamber outlet.

Many thermo-physical analyses were performed (TGA, elemental analyses, heat value measurements) to determine the properties of the biomasses used before the combustion stage (Bennini et al. 2019; Elorf et al. 2016; Rahib et al. 2021). As an example, Table 12.2 gives the elemental analysis results (C, H, N, S, O) and the caloric value for given samples of olive pomace and argan nut shells (ANS). Note

that the calorific value is high, which allows two biomasses to be a substitute for wood or coal in heat production systems. Elemental analysis gives high levels of carbon and oxygen and relatively low levels of hydrogen and nitrogen. No trace of sulfur is observed in these types of biomasses.

12.4.4.2 Combustion of Olive Pomace

Figure 12.4 illustrates examples of flames obtained according to the granulometry of olive pomace: raw particles (1–20 mm), medium size (1–5 mm), and fine size (<1 mm). It was observed that the flame develops better with raw- or medium-sized biomass compared to that obtained with fine particles. This is due probably to the high density of the biomass bed with the fine particles that somehow weakens the injection of air into the combustion zone, which leads to poor mixing between the reactants.

Figure 12.5 shows the maximum temperatures obtained as a function of AFR (air-fuel ratio) for the combustion of 1 kg of raw olive pomace. The Ti readings indicate values above 600 °C in the combustion products. These results are extremely

Fig. 12.4 Example of flames obtained according to the particle size of olive pomace
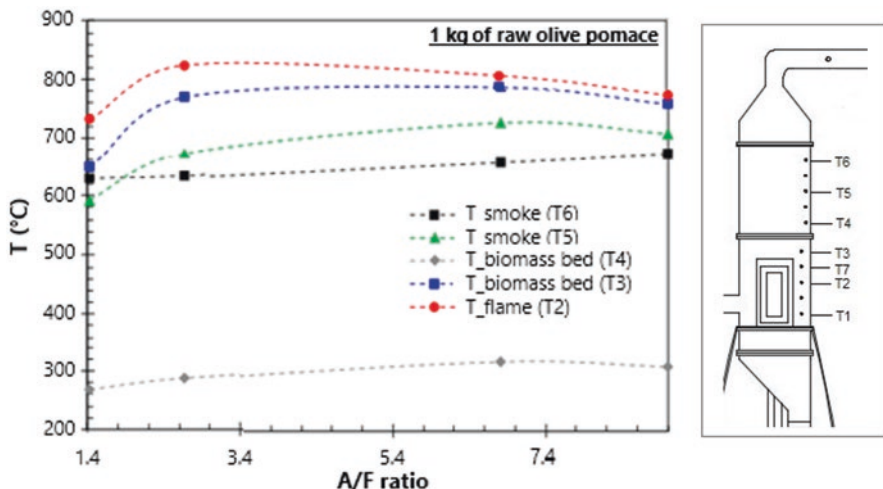
Fig. 12.5 Temperature variation according to the AFR (air-fuel ratio) at initial injection

Table 12.3 Variation of gas emissions according to AFR and particle sizes

Mass	0.5 kg raw pomace		0.5 kg medium particles		0.5 kg fine particles		
Total time (min)	09:00		10:00		13:00		
Measurement time	02:00	04:00	02:00	06:00	04:00	08:00	10:00
Air flow rate (m³/h)	10		9	22	8		21
AFR	3.5		3.5	8.7	3.5		10.7
$O_2\%$	7.1	13.7	11.4	15.8	…	…	…
$CO_2\%$	14.27	9.43	10.8	5.35	5.38	3.1	2.03
CO%	1.264	0.622	0.498	0.713	0.356	0.286	0.27
NO ppm	138	199	155.5	82	44	34	64
NO_2 ppm	2	0	9.5	9	18	40	10
NO_x ppm	139	199	165	91	61	75	74

promising for use in heating/DHW and eventually to produce steam which can be used with a micro turbine to produce electricity (Creyx et al. 2016).

Table 12.3 shows the evolution of pollutant emissions for three samples of olive pomace with different grain sizes: raw particles, medium-diameter particles (1–5 mm), and small-diameter particles (<1 mm). Experiments were conducted by sometimes varying the air flow (from rich to the lean regime), knowing that the stoichiometric AFR is estimated at 6.9. In general, relatively correct NO_x emissions are observed, between 50 and 200 ppm depending on the flow conditions, size of biomass, and measurement time. CO emissions globally are high, but the rate naturally decreases with excess air. These rates are usually obtained for biomass boilers. This high CO in the fumes is probably due to poor mixing in the biomass bed. The air would not necessarily pass through all the areas where biomass particles are

present on the perforated air inlet plate. It would be better to modify the air intake plate by making more holes with fewer gaps. Note that the combustion of this biomass visibly produces a lot of soot, given the color of the flame, the high presence of the CO level, and the recovery of small black particles at the level of the cyclone. The formation of soot depends strongly on the nature of the fuel, the behavior of the flame, and the local equivalence ratio (Desgroux et al. 2013) which is linked to input parameters such as the air flow rate and the size of particles.

Experiments were also done on argan nut shell biomass (ANS) as presented in Rahib et al. (2021).

12.5 Hydrothermal Carbonization (HTC)

12.5.1 General Concept

HTC is a process that uses water and heat to transform biomass or residues into carbon compounds (Fig. 12.6). This transformation results in decarboxylation and hydrolysis reactions but also polymerization reactions allowing the production of secondary hydrochar (Zhao et al. 2014). The biomass-to-water mass ratio can vary from 1:2 to 1:10, making it possible to work with wet residues such as sewage sludge, olive pomace, bagasse, and also fishery waste, algae, and animal waste. This hydrothermal treatment on wet residues avoids the drying phase needed in the case of pyrolysis or gasification or direct combustion of biomass.

Water plays the role of solvent, but HTC exploits the physicochemical properties of water which evolve with temperature. HTC is usually produced in closed reactors that produce autogenous pressure. Note that water at 180 °C has an equilibrium pressure of 1 MPa and about 4 MPa at 250 °C. The technology used should therefore take into account the rise in pressure. This pressure management makes HTC
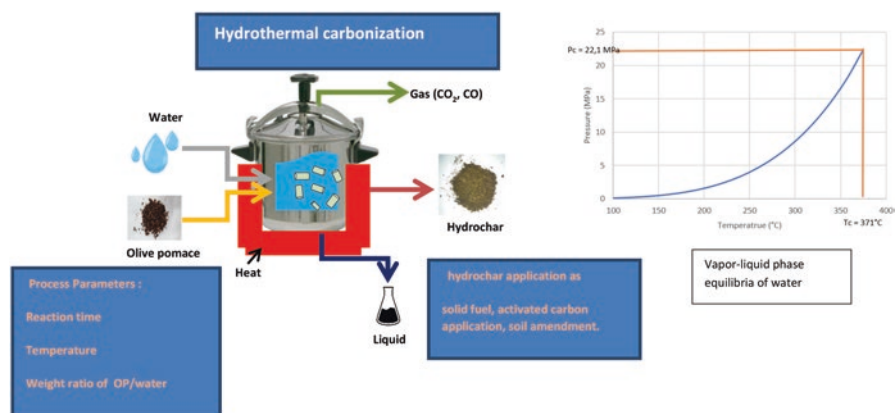

Fig. 12.6 Schematic illustration of the hydrothermal carbonization process

more constraining to gasification or pyrolysis. Furthermore, the water reaches supercritical conditions for a temperature of 371 °C and a pressure of 221 bars. Under these conditions, the density of water is about 0.3 g/cm³. This density is about 3 times less dense than water at 25 °C and about 1000 times denser than water in the vapor state at 1 bar. The ionization constant of the water can reach a value of 10^{-11} mol².kg⁻¹ corresponding to a value of 1000 times greater than that obtained at ambient temperature. This evolution increases the concentration of protons and free hydroxyl ions by 30 times, thus favoring catalytic reactions. Moreover, the evolution of the dielectric constant (ε) is surprisingly observed. This constant decreases to 2.5 at 250 bars and for a temperature of 400 °C giving it a polarity equivalent to that of acetone. These conditions allow solubilizing of the organic compounds (Kruse and Dinjus 2007).

Water also denatures plant cell walls and degrades the main biomass constituents which are hemicellulose, cellulose, and lignin. In the biomass compounds not mentioned, we have extractable compounds (which are soluble compounds in toluene or acetone according to the protocols put in place to quantify the three major compounds), proteins, lipids, and mineral compounds. The decomposition phases will be different depending on the chemical families. For the three main compounds, their decompositions are carried out by the first hydrolysis which will release molecules of lower molecular weight. Thus, α-cellulose (polymer consisting of glucose units bound together by alpha 1–4 bonds) decomposes into polysaccharides and hexoses (glucose, fructose). These oses then undergo dehydration to form furfurals and organic acids (Bobleter 1994; Wang et al. 2018). At the same time, these furfurals can condense to make polymers. These polymers will form secondary char (Sangare et al. 2022). For hemicellulose, the more complex polymer of pentoses xylose and hexoses, its decomposition pathways are quite similar, but the carbohydrate unit obtained is a pentose called xylose. In contrast to cellulose and hemicellulose, lignin has an aromatic structure based on three compounds: the p-coumaryl, coniferyl, and sinapyl alcohol. Thus, its decomposition path is different. In a simplified way, part of this lignin will solubilize in oligomers which will give phenolic compounds, and aldehydes. These compounds will form polymers giving an aromatic hydrochar. On the other hand, some of the lignin will not solubilize. This insoluble part is also a polyaromatic hydrocarbon similar to that obtained by pyrolysis, which may be called primary carbon. So, the contents of cellulose, hemicellulose, and lignin have a significant influence on the hydrochar porosity, surface functional group, and thermal stability. For example, this is observed during TG analyses, by the values of the characteristic peak of decomposition of hemicellulose which is around 295 °C; for cellulose 350 °C and for lignin, its characteristic peak is wider between 360 and 700 °C.

Moreover, hydrothermal treatments generate three different phases: a solid phase called hydrochar, an oil phase called biocrude or bio-oil, and a gas phase. In the range of process temperatures between 180 and 260 °C, the largest phase is solid. This is hydrothermal carbonization (HTC). For temperatures between 260 °C and the supercritical temperature (371 °C), the major phase will be the biocrude. This is hydrothermal liquefaction. Its application allows the production of biofuels that

must undergo treatment for their use (Deuber et al. 2021). Finally, for temperatures above the supercritical temperature, the main phase will be the gas whose composition will mainly be CO, CO_2, CH_4, and H_2 (syngas) which are the ultimate stage of decomposition of the main biomass compounds. It is the supercritical water gasification (SCWG) (Graz et al. 2016; Kruse 2008).

12.5.2 Potential Hydrochar Applications

In the context of the HTC, hydrochar has several ways of valorization which are the use as solid fuel, as an activated carbon, or as soil remediation.

12.5.2.1 Solid Fuel Application

To assess the quality of the hydrochars, the following combustion characteristics are used: the HHV (in MJ/kg), the volatile matter (VM), fixed carbon (FC), and ash fractions (in %) which are obtained owing to the proximate analysis. However, we can also determine the ignition (T_i), maximum reaction rate (T_m), and burnout temperature (T_b) by identifying the relevant point of (TG-DTG) analyses. T_i is associated with which the fuel is likely to self-ignite. T_b corresponds to the temperature stabilized for a rate loss of weight less than 1%/min when the sample is completely oxidized (Sangare et al. 2020; Zhang et al. 2020). Furthermore, a combustibility index (SN) can be expressed, and the more its value is high, the better the combustion characteristic.

12.5.2.2 Activated Carbon Application

Hydrochar has a great interest as carbon materials are used, for example, as absorbents for gas purification, water treatment, and energy storage. The textural properties of the activated carbon (AC) prepared from hydrochar were studied by N_2 and CO_2 gas adsorption to give the surface areas and the pore volumes. The treatments studied focus on their impact on their BET surface and the volume of pores generally. For instance, BET surface values of 673 m^2/g were obtained for hydrochar produced from glucose (Fechler et al. 2013).

12.5.2.3 Soil Amendment

The hydrochar can be used as a soil amendment to sequester carbon and enhance soil quality by improving the soil structure and the water retention and enhancing the cation exchange capacity. For example, studies have shown that poultry

litter-derived hydrochar seems to be an adequate amendment for sandy soils (Mau et al. 2020).

12.5.2.4 The Process Water (PW)

The HTC liquid treatment represents the largest mass of the outgoing effluent of HTC process. By reutilization of the PW, the amount of contaminated wastewater can be strongly reduced. However, the process temperature influences hydrochar and PW composition during PW recirculation. In the case of green municipal waste (MGW), the PW after HTC was fully reused up to 11 times (Köchermann et al. 2018). Results showed that hydrochar mass yield increases with progressing PW recirculation. However, the HHV was not affected by it. The liquid contains molecules such as furfurals and acids obtained from the degradation of the main components of biomass.

Some studies have examined the potential of PW for biochemical methane production. This liquid may also be a source of nitrogen and humic acid which improves soil fertility (Gupta et al. 2021). The process water can also be used for microalgae production and provides some necessary nutrients without inhibiting the growth of microalgae (Özçimen et al. 2022).

The fate of this water must be taken into account in the whole process. Furthermore, this water affects the energy balance of the process. In order to have a favorable balance, it is necessary to seek to work with the highest biomass/water mass ratio. In the case of olive pomace, it has been shown that this ratio must be at least equal to 1/5 in order to allow an energy balance favorable to the process (Missaoui et al. 2017a, b).

12.5.3 HTC Process

The three main operating parameters of HTC are the temperature (T), the reaction time (t), and the weight ratio biomass/water. Other factors may affect biomass degradation such as the feedwater pH and the concentration of substrate.

In the case of temperature and reaction time, there is an interaction between these two quantities. A conversion rate depends on the reaction time and its kinetics which varies with the temperature. So, some studies used a term of hydrothermal severity (R_0) which takes into account these two parameters.

$$R_0 = t \times \exp\left[(T - 100)/\omega\right]$$

(12.14)

with T = process temperature (°C); t = reaction time (min); ω is an empirical parameter that relates to the gas constant (R), the activation energy (E_a), and the reference temperature. Its value is equal to 14.75 when lignocellulosic biomasses are involved.

This term can be also called severity index (SI) expressed by the following equation:

$$\text{SI} = \int_{t}^{0} e^{\left(\frac{-E_a}{R}\right) \times \left(\frac{1}{T} - \frac{1}{T_0}\right)} \, \mathrm{d}t$$

(12.15)

with T_0 = reference temperature.

Most studies focus on the influence of T and t. For t, it is very variable, since it can range from 0 min to 24 h of treatment. In general, the longer the time increases, the lower the mass yield of the hydrocarbon, but the higher its HHV and its fixed carbon content.

To show these relations, the following application relates HTC processing of olive pomace collected from a three-phase centrifugation system of a semi-industrial unit in Morocco. In this application, the biomass/water mass ratio is 1/3. A Doelhert design was implemented in view to study the influence of T and t. The studied domain was for T between 180 and 250 °C and t between 0 and 60 min. In fact, $t = 0$ min corresponds to the time at which the solution remains at the desired temperature. $t = 0$ min allows showing the impact of the heating rate. Owing to Doelhert's design, we are able to represent the main effect graphic also the response surface modeled from factors on specific responses (as in Fig. 12.7) owing to a model as

$$Y = b_0 + b_1 X_1 + + b_2 X_2 + b_{11} X_{12} + + b_{22} X_{22} + + b_{12} X_1 X_2$$

(12.16)

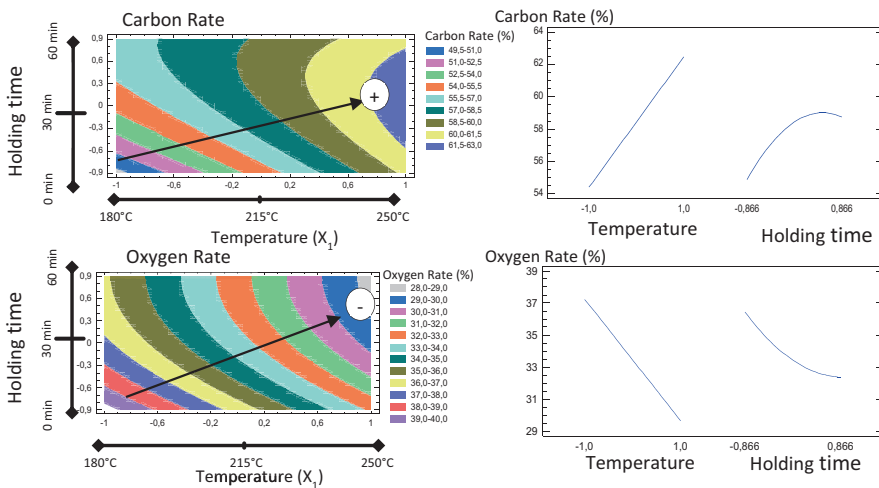With X_i factors, Y response and b_i model coefficients.

Fig. 12.7 The main effects (on the right) and 2D contour plots (on the left) of temperature and holding time on carbon and oxygen rates

Figure 12.7 reveals that the carbon rate increases with t and T contrary to the oxygen rate. So, the ratio O/C decreases with increasing factors favorable pour fuel application. The same trend is shown with the HHV allowing to have a value of 20% greater than the raw olive pomace. On the other hand, the hydrochar mass yield decreases to a minimum value of 66%.

The energy efficiency (EY) makes it possible to take into account this antagonistic evolution by the fact that its calculation is carried out with the following formula:

$$EY\,(\%) = Mass\ yield \times Densification\ energy\ ratio \tag{12.17}$$

and densification energy ratio:

$$DE\,(-) = \frac{HHV_{\text{dried hydrochar}}}{HHV_{\text{dried olive pomace}}} \tag{12.18}$$

The EY values were between 80% and 92%. Moreover, the energy balance, which takes into account the energy recovery minus the energy consumption, can be considered positive in all the domains favoring the introduction of such a process.

12.6 Characterization of Gaseous Products Evolved from Biomass Fuels During Thermochemical Conversion Using TGA-µGC

12.6.1 Introduction

The production of new clean and sustainable fuels from biomass thermochemical conversion has enhanced the demand for in-depth characterization of the evolved gases upon thermal decomposition. In order to apply these processes, the thermal degradation must be properly characterized for mass loss, temperature, and the nature and composition of the gases evolved during the thermal conversion of biomass.

Thermogravimetric analysis (TGA) coupled with micro-gas chromatography (micro-GC or µGC) allows determining precisely and in a short time the key parameters required for the process design of thermochemical conversion technologies.

This section describes a practical application of the thermal degradation of two biomass wastes in a Netzsch TGA instrument coupled with a 3-module micro-gas chromatograph (SRA Instruments), and the results presented illustrate the investigation of fuel production from olive pomace (OP) and miscanthus.

12.6.2 Theory and Operating Principles of TGA and Simultaneous Evolved Gas Analysis

12.6.2.1 Thermogravimetric Analysis

TGA is a thermo-analytical technique that combines gravimetric measurements with furnace heating to measure the mass of a sample as a function of temperature in a defined atmosphere (Dunn 2002). The sample (usually a solid) undergoes thermal degradation and subsequent gas–solid heterogeneous reactions that result in the evolution of gaseous, liquid (tars), and residue by-products. In TGA, the gaseous products are removed by a flowing gas, and the changes in the remaining mass of the sample can be presented in two different plots, as depicted in Fig. 12.8a.

Gasifying agent: air at an equivalence ratio of 0.20 from 700 to 1000 °C. (a) TGA curves and black and red (solid) lines represent the TG and DTG profiles, respectively. (b) Main volatile decomposition products over time and temperature, dash-dotted line: temperature program from room temperature to 1000 °C; color lines: releasing profile of target gas products (CO, CO_2, CH_4, and H_2).

The thermogravimetric (TG) curve (in wt.%) is a plot of the mass of the sample against time or temperature. Similarly, the derivative of TGA data can be plotted as a derivative thermogravimetric (DTG) curve (in wt.%/min or wt.%/°C), which is a plot of the rate of change of mass with respect to temperature or time against temperature or time (Dunn 2002). This allows for the determination of mass-loss stages and specific decomposition temperatures, such as the temperature of the maximum rate of mass loss (T_{max}) at which the material decomposes or reacts (DTG peak). Onset (ignition, T_i) and final (burnout, T_b) degradation temperature data can also be evaluated from TG plots (ASTM 2011; Sangare et al. 2020).

Therefore, TGA is extensively used for assessing the reactivity phenomena involving biomass and solid wastes. It can provide valuable information on compositional changes and enables a wide range of experimental conditions (i.e., sample
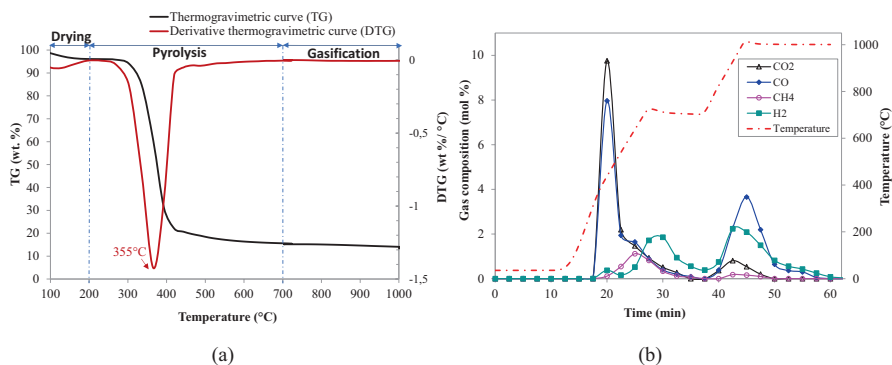

(a)   (b)

Fig. 12.8 Thermogravimetric and evolved gas analysis of the pyrolysis-char gasification process of cellulose upon heating at 40 °C/min. Char resulting from cellulose pyrolysis at 700 °C in flowing argon (20 mL/min)

mass, heating rate, specific atmosphere, final temperature, holding time, nature, and flow rate of the reactive gas) to be adapted to the feedstock composition to which TGA is applied, which is done through analysis of characteristic TG and/or DTG profiles (Fig. 12.8a).

Furthermore, detailed information like moisture loss and volatile matter (VM), fixed carbon (FC), and ashes content can also be determined using TGA standardized analytical procedures (ASTM 2014).

12.6.2.2   Simultaneous Thermogravimetric and Micro-Gas Chromatography (TGA-μGC) Analysis

TGA can be used simultaneously or separately, depending on the research objective, for the analysis of dehydration, thermal decomposition, oxidization, and other processes which are involved in the energy conversion of biomass and waste management. By combining TGA with other analytical methods, additional information can be obtained from one sample. In particular, TGA coupled with micro-GC enables both qualitative and quantitative analyses of biomass and organic waste samples.

The operation principle of a micro-GC analysis system is based on miniaturized chromatographic separations to provide rapid and in situ characterization in gas mixtures (Regmi and Agad 2018). The composition of evolved gases enriched in hydrogen (H_2), carbon monoxide (CO), and methane (CH_4) can be studied by micro-GC analysis (Fushimi et al. 2003; Xu et al. 2011, 2020; Yang et al. 2007; Zhu et al. 2018). Carbon dioxide (CO_2), nitrogen (N_2), and oxygen (O_2), if released, can also be detected and quantified.

Figure 12.9 summarizes the flow of operating procedure of the TGA-μGC system. Simultaneous TGA and micro-GC measurements are carried out in three steps: *(i)* the sample is first heated on the TGA, *(ii)* the evolved gaseous effluent is directed to the micro-GC through the transfer line, *(iii)* the target gas species eluting from the micro-GC columns are identified and quantified by comparing the peak area signal and retention times with those of calibration standards under the same conditions as the samples. The thermogravimetric and chromatographic data are continuously recorded on a computer over the course of the experimental run.
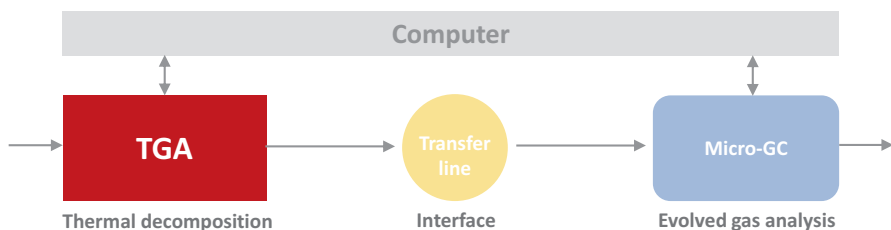

Fig. 12.9   TGA and micro-GC coupling principle

The experimental setup consists of a Netzsch STA 449 F3 Jupiter thermogravimetric analyzer coupled with a micro-gas chromatograph (Micro GC SOLIA 490, SRA Instruments). The micro-GC device is equipped with micro-packed columns and three thermal conductivity detector (TCD) channels. The experimental procedures were based on the methodology developed by Sangaré et al. (2022). The TGA-μGC coupling requires the synchronization of the operating conditions of both instrumental devices. The setup optimization was obtained by following manufacturers' specifications for the Solia 490 micro-GC and performing preliminary TGA-μGC measurements on cellulose as a reference case. The micro-GC starts with the TGA at the beginning of the run, and the complete gas composition is obtained in less than 3 min (~150 s analysis time) for H_2, CH_4, CO, and CO_2, by optimizing the heating rate, final temperature, and carrier gas (type and flow rate) experimental conditions. Three consecutive runs were conducted, which demonstrated a maximum standard deviation of less than 2.3% for the peak area of all compounds of interest. The detailed operating conditions can be found elsewhere (Sangaré et al. 2022).

As an example, the pyrolysis and gasification outputs of cellulose under argon and air atmospheres are presented in Fig. 12.8. Firstly, a dehydration stage took place due to evaporation of moisture below 150 °C. This was followed by a primary pyrolysis step that produces char, followed by air gasification of that char from 700 to 1000 °C with an equivalence ratio of 0.20. A single mass-loss stage in the temperature range between 300 and 415 °C, and a maximum decomposition rate (1.42 wt.%/°C) was reached at ~355 °C (DTG peak), which is in agreement with the results reported in the literature (Yang et al. 2007). The devolatilization rate shows that cellulose is converted mainly to volatiles. Approximately 85 wt.% of cellulose was devolatilized up to 700 °C (Fig. 12.8a). To quantitatively characterize the effect of temperature on gas release, the analysis of the gas evolution over time and temperature was made by online TGA-μGC measurements.

Figure 12.8b shows the effects of pyrolysis and gasification temperature on the composition of gas products of cellulose. CO, CO_2, H_2, and CH_4 are the main gas products. The content of CO, CO_2, H_2, and CH_4 in the pyrolysis gases accounted for more than 36 mol%. As the temperature increased, the H_2 content in the product gases increased from 5.83 mol% at 700 °C to 8.31 mol% at 1000 °C, while CO, CO_2, and CH_4 evolution exhibited the opposite trend. The H_2/CO ratio was increased from 0.45 to 0.87 at 700 °C and 1000 °C, respectively. The lower heating value (LHV) of the product gases from cellulose was 6.5 MJ/Nm^3, as estimated by Xie et al. (2012).

TGA-μGC coupling is considered to be an effective technique to identify and easily quantify the main compounds causing a mass loss during thermal decomposition. The resulting data can contribute to determining the utilization of a biomass sample or mixture as an energy source in thermochemical processes or other applications.

In the following, a comparative case is presented to support biomass and waste management valorization opportunities using thermochemical conversion technologies for social development in rural areas of developing countries.

12.6.3 Case Study

Two examples are presented to illustrate the simultaneous characterization of biomass thermal decomposition and analysis of the evolved gas, in a single run, using TGA-µGC coupling.

The first is the gasification of olive pomace (OP), and the other is the gasification of miscanthus. In terms of waste characteristics, the proximate analysis, ultimate analysis, and heating values of miscanthus and OP are given in Table 12.4. The OP composition is almost comparable with miscanthus. So, OP and miscanthus opted for the present comparative study.

The influence of the feedstock type on the gasification process through TGA of the biomass samples is depicted in Fig. 12.10. As can be seen in this figure, both samples involve a major mass loss step that occurred at 250–415 °C, with approximately 30% of solid residue left for the OP and 20% for miscanthus at 1000 °C. The DTG showed a maximum weight loss rate (0.80 wt.%/°C) at 350 °C for OP, and two observable peaks (~1.51 and 0.92 wt.%/°C) attained for miscanthus at 325 °C and 365 °C, respectively. This suggests that this region could be divided into two stages corresponding to different thermochemical reactions, in which the main weight loss is due to removal of the volatile matters of the biomass. In both cases, the differences in the intrinsic chemical and structural features of the two biomass samples possibly account for the different gasification behaviors observed (McKendry 2002; Yang et al. 2007).

The gas data in Fig. 12.10 show that the CO_2 evolved during gasification was lower for miscanthus, while CO production was increased and CH_4 and H_2 were
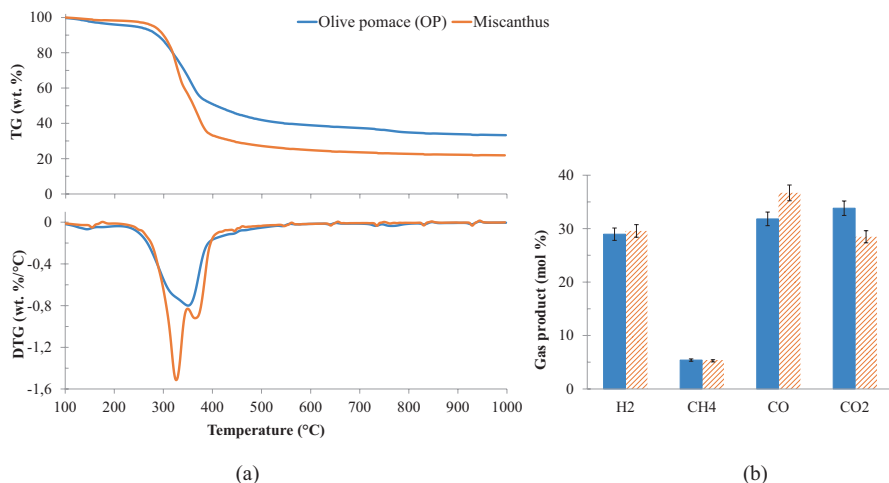

(a)   (b)

Fig. 12.10 Thermogravimetric and evolved gas analysis of the gasification process of OP and miscanthus upon heating at 40 °C/min in flowing nitrogen (20 mL/min). Gasifying agent: air at an equivalence ratio of 0.10 from 110 to 1000 °C. (**a**) TGA curves: TG and DTG profiles, respectively. (**b**) Main gas products (H_2, CH_4, CO, and CO_2)

much similar for both study cases. The produced gases had a LHV of 9.1 MJ/Nm^3 and 9.7 MJ/Nm^3, respectively, for OP and miscanthus, at this temperature range (250–1000 °C).

12.6.4 Summary

The measurements presented show that the combination of TGA and micro-GC analyses allows determining accurately (±2.3% standard deviation) and in a short time (~150 s analysis time) the amounts of the target gases, such as H_2, CH_4, CO, and CO_2, produced during the pyrolytic and gasification processes. The pyrolysis of cellulose was used here as an example. Under similar measurement conditions, within one test series, a comparative evaluation of the gasification products of OP and miscanthus was presented. The effect of measurement conditions, including temperature, heating rate, feedstock composition, and blending ratios, as well as the type and flow rate of the carrier gas must be considered when performing simultaneous TGA-μGC studies. Finally, the proposed methodology can contribute to expanding the analytical techniques used in thermochemistry and broaden the assessment of waste sources for the production of synthetic fuels in developing countries.

References

ASTM, *ASTM E2550-11, Standard Test Method for Thermal Stability by Thermogravimetry* (West Conshohocken, 2011)

ASTM, *ASTM E1131–08, Standard Test Method for Compositional Analysis by Thermogravimetry* (West Conshohocken, 2014)

M.A. Bennini, A. Koukouch, I. Bakhattar, M. Asbik, T. Boushaki, B. Sarh, et al., Characterization and combustion of olive pomace in a fixed bed boiler: Effects of particle sizes. Int. J. Heat Technol. **37**, 229–238 (2019). https://doi.org/10.18280/ijht.370128

O. Bobleter, Hydrothermal degradation of polymers derived from plants. Prog. Polym. Sci. **19**, 797–841 (1994). https://doi.org/10.1016/0079-6700(94)90033-7

M. Creyx, E. Delacourt, C. Morin, S. Lalot, B. Desmet, Energetic and exergetic analysis of a heat exchanger integrated in a solid biomass-fuelled micro-CHP system with an Ericsson engine. Entropy **18** (2016). https://doi.org/10.3390/e18040154

A. Demirbas, Combustion of biomass. Energy Source A Recover Util. Environ. Eff. **29**, 549–561 (2007). https://doi.org/10.1080/009083190957694

P. Desgroux, X. Mercier, K.A. Thomson, Study of the formation of soot and its precursors in flames using optical diagnostics. Proc. Combust. Inst. **34**, 1713–1738 (2013). https://doi.org/10.1016/j.proci.2012.09.004

R.D.S. Deuber, D.S. Fernandes, J.M. Bressanin, J. Watson, M.F. Chagas, A. Bonomi, et al., Techno-economic assessment of HTL integration to the Brazilian sugarcane industry: An evaluation of different scenarios. Ind. Crop. Prod. **173** (2021). https://doi.org/10.1016/j.indcrop.2021.114139

J. Dunn, Thermogravimetric analysis, in *Characterization of Materials*, ed. by E.N. Kaufmann, (The University of Toledo, Toledo, 2002)

A. Elorf, N.M. Koched, T. Boushaki, B. Sarh, J. Chaoufi, S. Bostyn, et al., Swirl motion effects on flame dynamic of pulverized olive cake in a vertical furnace. Combust. Sci. Technol. **188**, 1951–1971 (2016). https://doi.org/10.1080/00102202.2016.1214419

A. Elorf, J. Kandasamy, V. Belandria, S. Bostyn, B. Sarh, I. Gökalp, Heating rate effects on pyrolysis, gasification and combustion of olive waste. Biofuels **12**, 1157–1164 (2021). https://doi.org/10.1080/17597269.2019.1594598

R.J. Evans, T.A. Milne, Molecular characterization of pyrolysis of biomass. 1. Fundamentals. Energy Fuel **1**, 123–138 (1987)

N. Fechler, S.A. Wohlgemuth, P. Jäker, M. Antonietti, Salt and sugar: Direct synthesis of high surface area carbon materials at low temperatures via hydrothermal carbonization of glucose under hypersaline conditions. J. Mater. Chem. A **1**, 9418–9421 (2013). https://doi.org/10.1039/c3ta10674h

C. Fushimi, K. Araki, Y. Yamaguchi, A. Tsutsumi, Effect of heating rate on steam gasification of biomass. 2. Thermogravimetric-mass spectrometric (TG-MS) analysis of gas evolution. Ind. Eng. Chem. Res. **42**, 3929–3936 (2003). https://doi.org/10.1021/ie0300575

C. Gai, Y. Dong, Experimental study on non-woody biomass gasification in a downdraft gasifier. Int. J. Hydrog. Energy **37**, 4935–4944 (2012). https://doi.org/10.1016/j.ijhydene.2011.12.031

J.R. Grace, B. Leckner, J. Zhu, J.R. Grace, Fluidized beds, in *Multiphase Flow Handbook*, ed. by C.T. Crowe, (CRC Press, New York, 2006)

Y. Graz, S. Bostyn, T. Richard, P.E. Bocanegra, E. De Bilbao, J. Poirier, et al., Hydrothermal conversion of Ulva macro algae in supercritical water. J. Supercrit. Fluids **107**, 182–188 (2016). https://doi.org/10.1016/j.supflu.2015.07.038

D. Gupta, S.M. Mahajani, A. Garg, Hydrothermal carbonization of household wet waste – Characterization of hydrochar and process wastewater stream. Bioresour. Technol. **342**, 125972 (2021). https://doi.org/10.1016/j.biortech.2021.125972

J.O. Ighalo, F.U. Iwuchukwu, O.E. Eyankware, K.O. Iwuozor, K. Olotu, O.C. Bright, et al., Flash pyrolysis of biomass: A review of recent advances. Clean Techn. Environ. Policy, 1–15 (2022)

IRENA, *Renewable Power Generation Costs in 2019 – Key Findings* (International Renewable Energy Agency, 2020), p. 160

K. Jayaraman, I. Gökalp, Pyrolysis, combustion and gasification characteristics of miscanthus and sewage sludge. Energy Convers. Manag. **89**, 83–91 (2015). https://doi.org/10.1016/j.enconman.2014.09.058

A.A. Khan, W. de Jong, P.J. Jansens, H. Spliethoff, Biomass combustion in fluidized bed boilers: Potential problems and remedies. Fuel Process. Technol. **90**, 21–50 (2009). https://doi.org/10.1016/j.fuproc.2008.07.012

D.L. Klass, *Biomass for Renewable Energy, Fuels, and Chemicals* (Academic, London, 1998). https://doi.org/10.5860/choice.36-4508

J. Köchermann, K. Görsch, B. Wirth, J. Mühlenberg, M. Klemm, Hydrothermal carbonization: Temperature influence on hydrochar and aqueous phase composition during process water recirculation. J. Environ. Chem. Eng. **6**, 5481–5487 (2018). https://doi.org/10.1016/j.jece.2018.07.053

A. Kruse, Supercritical water gasification. Biofuels Bioprod. Biorefining Innov. Sustain. Econ. **2**, 415–437 (2008)

A. Kruse, E. Dinjus, Hot compressed water as reaction medium and reactant. Properties and synthesis reactions. J. Supercrit. Fluids **39**, 362–380 (2007). https://doi.org/10.1016/j.supflu.2006.03.016

P.S. Lam, S. Sokhansanj, X. Bi, C.J. Lim, L.J. Naimi, M. Hoque, et al., Bulk density of wet and dry wheat straw and switchgrass particles. Appl. Eng. Agric. **24**, 351–358 (2008)

C. Mandl, I. Obernberger, F. Biedermann, Modelling of an updraft fixed-bed gasifier operated with softwood pellets. Fuel **89**, 3795–3806 (2010). https://doi.org/10.1016/j.fuel.2010.07.014

V. Mau, G. Arye, A. Gross, Poultry litter hydrochar as an amendment for sandy soils. J. Environ. Manag. **271**, 110959 (2020). https://doi.org/10.1016/j.jenvman.2020.110959

P. McKendry, Energy production from biomass (part 1): Overview of biomass. Bioresour. Technol. **8**, 37–46 (2002)

T.A. Milne, A.H. Brennan, B.H. Glenn, *Sourcebook of Methods of Analysis for Biomass and Biomass-Conversion Process* (Elsevier, London, 1990)

A. Missaoui, S. Bostyn, V. Belandria, B. Cagnon, B. Sarh, I. Gökalp, Hydrothermal carbonization of dried olive pomace: Energy potential and process performances. J. Anal. Appl. Pyrolysis **128**, 281–290 (2017a). https://doi.org/10.1016/j.jaap.2017.09.022

A. Missaoui, S. Bostyn, V. Belandria, B. Sarh, I. Gökalp, *Assessing the Heat and Energy Balances of Hydrochar Production via Hydrothermal Carbonization of Olive Pomace*. In 25th European biomass conference exhibition (2017b)

T. Nussbaumer, Combustion and co-combustion of biomass: Fundamentals, technologies, and primary measures for emission reduction. Energy Fuel **17**, 1510–1521 (2003). https://doi.org/10.1021/ef030031q

D. Özçimen, B. Inan, A.T. Koçer, S. Bostyn, I. Gökalp, Hydrothermal carbonization processes applied to wet organic waste streams. Int. J. Energy Res. (2022). https://doi.org/10.1002/er.8304

T.K. Patra, P.N. Sheth, Biomass gasification models for downdraft gasifier: A state-of-the-art review. Renew. Sust. Energ. Rev. **50**, 583–593 (2015). https://doi.org/10.1016/j.rser.2015.05.012

L. Pelkmans, *IEA Bioenergy Countries' Report-Update 2021: Implementation of Bioenergy in the IEA Bioenergy Member Countries* (2021), pp. 1–28

Y. Rahib, T. Boushaki, B. Sarh, J. Chaoufi, Combustion and pollutant emission characteristics of argan nut shell (ANS) biomass. Fuel Process. Technol. **213**, 106665 (2021). https://doi.org/10.1016/j.fuproc.2020.106665

B.P. Regmi, M. Agah, Micro gas chromatography: An overview of critical components and their integration. Anal. Chem. **90**, 13133–13150 (2018)

Y. Rogaume, *La combustion du bois et de la biomasse*. Pollut Atmosphérique, Clim Santé, Société (2009); Numéro spé:65–82.

L. Rosendahl (ed.), *Biomass Combustion Science, Technology and Engineering* (Woodhead Publishing, Oxford, 2013)

D. Sangare, A. Missaoui, S. Bostyn, V. Belandria, M. Moscosa-Santillan, I. Gökalp, Modeling of Agave Salmiana bagasse conversion by hydrothermal carbonization (HTC) for solid fuel combustion using surface response methodology. AIMS Energy **8**, 538–562 (2020)

D. Sangaré, S. Bostyn, M. Moscosa Santillán, P. García-Alamilla, V. Belandria, I. Gökalp, Comparative pyrolysis studies of lignocellulosic biomasses: Online gas quantification, kinetics triplets, and thermodynamic parameters of the process. Bioresour. Technol. **346** (2022). https://doi.org/10.1016/j.biortech.2021.126598

D. Sangare, A. Chartier, M. Moscosa-Santillan, I. Gökalp, S. Bostyn, Kinetic studies of hydrothermal carbonization of avocado stone and analysis of the polycyclic aromatic hydrocarbon contents in the hydrochars produced. Fuel **316** (2022). https://doi.org/10.1016/j.fuel.2022.123163

S.K. Sansaniwal, K. Pal, M.A. Rosen, S.K. Tyagi, Recent advances in the development of biomass gasification technology: A comprehensive review. Renew. Sust. Energ. Rev. **72**, 363–384 (2017). https://doi.org/10.1016/j.rser.2017.01.038

I.P. Silva, R.M.A. Lima, G.F. Silva, D.S. Ruzene, D.P. Silva, Thermodynamic equilibrium model based on stoichiometric method for biomass gasification: A review of model modifications. Renew. Sust. Energ. Rev. **114**, 109305 (2019). https://doi.org/10.1016/j.rser.2019.109305

P. Sommersacher, T. Brunner, I. Obernberger, Fuel indexes: A novel method for the evaluation of relevant combustion properties of new biomass fuels. Energy Fuel **26**, 380–390 (2012). https://doi.org/10.1021/ef201282y

D.A. Tillman, Biomass combustion, in *Biomass Regeneration Energy*, ed. by D.O. Hall, R.P. Overend, (Wiley, New York, 1987), pp. 203–219

M.L. Valderrama Rios, A.M. González, E.E.S. Lora, O.A. Almazán del Olmo, Reduction of tar generated during biomass gasification: A review. Biomass Bioenergy **108**, 345–370 (2018). https://doi.org/10.1016/j.biombioe.2017.12.002

J.M. Vargas-Moreno, A.J. Callejón-Ferre, J. Pérez-Alonso, B. Velázquez-Martí, A review of the mathematical models for predicting the heating value of biomass materials. Renew. Sust. Energ. Rev. **16**, 3065–3083 (2012). https://doi.org/10.1016/j.rser.2012.02.054

T. Wang, Y. Zhai, Y. Zhu, C. Li, G. Zeng, A review of the hydrothermal carbonization of biomass waste for hydrochar formation: Process conditions, fundamentals, and physicochemical properties. Renew. Sust. Energ. Rev. **90**, 223–247 (2018). https://doi.org/10.1016/j.rser.2018.03.071

J. Watson, Y. Zhang, B. Si, W.T. Chen, R. de Souza, Gasification of biowaste: A critical review and outlooks. Renew. Sust. Energ. Rev. **83**, 1–17 (2018). https://doi.org/10.1016/j.rser.2017.10.003

Q. Xie, S. Kong, Y. Liu, H. Zeng, Syngas production by two-stage method of biomass catalytic pyrolysis and gasification. Bioresour. Technol. **110**, 603–609 (2012)

Q. Xu, S. Pang, T. Levi, Reaction kinetics and producer gas compositions of steam gasification of coal and biomass blend chars, part 1: Experimental investigation. Chem. Eng. Sci. **66**, 2141–2148 (2011). https://doi.org/10.1016/j.ces.2011.02.026

D. Xu, Y. Xiong, J. Ye, Y. Su, Q. Dong, S. Zhang, Performances of syngas production and deposited coke regulation during co-gasification of biomass and plastic wastes over Ni/γ-Al$_2$O$_3$ catalyst: Role of biomass to plastic ratio in feedstock. Chem. Eng. J. **392**, 123728 (2020). https://doi.org/10.1016/j.cej.2019.123728

H. Yang, R. Yan, H. Chen, D.H. Lee, C. Zheng, Characteristics of hemicellulose, cellulose and lignin pyrolysis. Fuel **86**, 1781–1788 (2007). https://doi.org/10.1016/j.fuel.2006.12.013

D. Yogi Goswami, F. Kreith, *Energy Conversion* (2008). https://doi.org/10.1007/978-3-030-56164-2_7

X. Zhang, Y. Li, M. Wang, L. Han, X. Liu, Effects of hydrothermal carbonization conditions on the combustion and kinetics of wheat straw hydrochar pellets and efficiency improvement analyses. Energy Fuel **34**, 587–598 (2020). https://doi.org/10.1021/acs.energyfuels.9b03754

P. Zhao, Y. Shen, S. Ge, K. Yoshikawa, Energy recycling from sewage sludge by producing solid biofuel with hydrothermal carbonization. Energy Convers. Manag. **78**, 815–821 (2014). https://doi.org/10.1016/j.enconman.2013.11.026

L. Zhu, Y. Zhang, H. Lei, X. Zhang, L. Wang, Q. Bu, et al., Production of hydrocarbons from biomass-derived biochar assisted microwave catalytic pyrolysis. Sustain. Energy Fuels **2**, 1781–1790 (2018). https://doi.org/10.1039/c8se00096d